Materials Characterization 118 (2016) 431–437

Contents lists available at ScienceDirect

Materials Characterization

journal homepage: www.elsevier.com/locate/matchar

In-situ EBSD study of deformation behavior of retained austenite in a low-carbon quenching and partitioning steel via uniaxial tensile tests

Wan-song Li [a], Hong-ye Gao [b], Hideharu Nakashima [c], Satoshi Hata [c], Wen-huai Tian [a,*]

[a] School of Materials Science and Engineering, University of Science and Technology Beijing, Beijing 100083, China
[b] Faculty of Engineering, Kyushu University, Fukuoka 8168580, Japan
[c] Interdisciplinary Graduate School of Engineering Sciences, Kyushu University, Fukuoka 8168580, Japan

ARTICLE INFO

Article history:
Received 28 February 2016
Received in revised form 8 June 2016
Accepted 16 June 2016
Available online 19 June 2016

Keywords:
Electron back-scattered diffraction
Grain rotation
Transformation
True strain

ABSTRACT

Through using in-situ electron back-scattered diffraction and uniaxial tensile tests, this work mainly focuses on the deformation behavior of retained austenite (RA) in a low-carbon quenching and partitioning (Q&P) steel. In this paper, three different types of RA can be distinguished from different locations, respectively, RA grains at the triple edges, twinned austenite and RA grains positioned between martensite. The results have shown that grains at the triple edges and twinned austenite could transform easily with increasing strain, i.e. are less stable when compared with RA grains distributed between martensite that could resist a larger plastic deformation. Meanwhile, the strain leads to rotations of RA grains distributed at the triple edges and between martensite. Moreover, RA grains with a similar orientation undergone similar rotations with the same true strain. These RA grains rotated along a specific slip plane and slip direction and the grain rotation is taken as a significant factor to improve the ductility of steel. In addition, grain sizes of RA decreased gradually with an increase of true strain and smaller (0–0.2 μm) grains were more capable of resisting the deformation. According to kernel average misorientation (KAM) analysis, it can be found that strain distribution is preferentially localized near martensite–austenite phase boundaries and in the interior of martensite. The average KAM values increased continuously with increasing true strain.

1. Introduction

Conventional transformation-induced plasticity (TRIP) steel is a kind of advanced high strength steel, including bainite, ferrite and retained austenite (RA). Because of the TRIP effect during deformation, RA transforms into martensite, which can significantly strengthen the matrix as well as improve the formability and energy absorption of TRIP steel [1]. Therefore, TRIP steel presents a good combination of strength and formability. Recently, Speer et al. proposed a novel and promising heat treatment process named quenching and partitioning (Q&P) [2,3]. The steel employed with the Q&P process exhibits a better comprehensive property than TRIP steel does [1].

Following aspects are involved in the Q&P process: (1) an isothermal treatment at the intercritical temperature or above Ac_3 for partial or full austenitization; (2) a rapid quenching at a given temperature between martensite-start (M_s) temperature and martensite-finish (M_f) temperature, so that a certain fraction of austenite can be formed; (3) a subsequent partitioning at the same or a higher temperature, so that the diffusion of carbon from martensite to austenite can be completed, which is conducive to the stabilization of the austenite at room temperature during the final cooling.

Various microstructure dependencies of the deformation behaviors have different effects on the mechanical properties of the material. Therefore, understanding the microstructural characteristics is useful to the optimization of the steel's mechanical properties. According to the investigations in TRIP steel, the deformation stability of RA is influenced by following factors: (i) the grain size of RA [4,5]; (ii) the local carbon content in RA [6]; (iii) the morphology [7,8]; (iv) the crystallographic orientation of RA relevant to the loading direction [6,9]; and (v) the constraining effect exerted by surrounding phases on RA [10, 11]. Also, these effects are considered as the main influencing factors of the deformation stability of RA in Q&P steel [12,13]. According to previous studies on Q&P steel [13,14], the RA grain can rotate to accommodate to plastic deformation during the strain. At the same time, the blocky RA grain is less stable than the film-like RA grain under the deformation [15]. In addition, the effect of strain distribution on the mechanical behavior in Q&P steel after partial austenitization has been investigated [16]. The result shows that the constraining effect of the fresh martensite on the strain distribution exerts a negative impact on the transformation stability of RA with increasing strain [11]. According to the different distribution, RA can be clarified into three types, i.e. film-like RA, blocky RA and twinned austenite. Nevertheless, a complete

* Corresponding author at: Room 303, Ceshi Building, University of Science and Technology Beijing, Xueyuan Road No. 30, Haidian District, Beijing 100083, China.
E-mail address: wenhuaitian@ustb.edu.cn (W. Tian).

http://dx.doi.org/10.1016/j.matchar.2016.06.020

understanding of the transformation mechanism of each type of RA in Q&P steel has not been obtained so far.

The purpose of this work is to better understand the transformation behavior of each type of RA in Q&P steel upon uniaxial deformation through in-situ electron backscatter diffraction (EBSD) measurements and tensile tests. Therefore, the transformation behavior of RA is analyzed based on the RA grain size, phase transformation, grain rotation as well as local strain distribution during the strain.

2. Experimental

The material investigated in this study is TRIP-assisted steel, the chemical composition of which is Fe-0.176C-1.31Si-1.58Mn-0.26Al-0.3Cr (in wt%). Firstly, a vacuum induction furnace was used to heat the steel at 1200 °C for 2 h, following which the steel was hot rolled to 6 mm in thickness. The transformation temperatures Ac_1, Ac_3 and M_s of the steel are 728 °C, 872 °C and 382 °C, respectively, which were calculated via the Thermo-Calc [17]. Moreover, all of the experimental specimens were cut from the plate along the rolling direction. As for the Q&P heat treatment, the specimen was fully austenitized at 900 °C for 300 s, and then quenched to 240 °C for 15 s in a salt bath. Next, the specimen was partitioned at 420 °C for 20 s in another salt bath and finally cooled in water.

The specimen used for the uniaxial tensile tests was prepared by an electric discharge machine, and its long axis was kept paralleling to the rolling direction of Q&P steel. The specific dimensions of the tensile specimen are shown in Fig. 1, and both the uniaxial tensile tests and in-situ EBSD experiments were carried out on the Zeiss Ultra 55 scanning electron microscope (SEM) equipped with a tensile tester. Prior to the EBSD analysis, the tensile specimen was mechanically lapped and polished with the conventional method, and then it was etched with 4% nital. Subsequently, the specimen was polished by a colloidal silica suspension with a particle diameter of 50 nm. Afterwards, the tensile specimen was marked with two small Vickers indentations to serve as the reference point of the EBSD patterns, as shown in Fig. 1. In addition, two indentations were kept 1 mm apart and the observed area of EBSD was performed on the center point of the specimen.

The strain rate in the uniaxial tensile test was set at ~2×10^{-5}/s. The EBSD data were obtained on the hexagonal scan grids with an accelerating voltage of 15 kV, a tilt angle of 70°, a working distance of 10 mm and a step size of 80 nm. The corresponding orientation data were post-processed with the OIM 6.0 software, which was supported by the EDAX Incorporation.

3. Results and discussion

3.1. Macroscopic stress–strain responses

Fig. 2 shows the macroscopic stress–strain curve of the specimen measured step-wisely in the strain control mode during in-situ (interrupted) EBSD experiment. Once a desired strain value was reached, the loading would be suspended, and then a small load drop could be observed. After each small load drop became stable, the EBSD experiment would be conducted. The true strains, which are calculated by measuring the distance between indentations (as shown in Fig. 1) after each tensile test, are listed in Table 1. As a comparison, another ex-situ (continuous) tensile test of a second specimen was also performed. The results of the in-situ and ex-situ tensile test are shown in Table 2. It is revealed from Table 2 that these two specimens differ to some extent in mechanical properties. In particular, the strength of the continuous tensile specimen seems to be higher. The reason for the systematic difference is not clear, but should be related to strain rate dependence or slight differences in the loading way on the deformation rigs applied to on- and off-line testing [18].

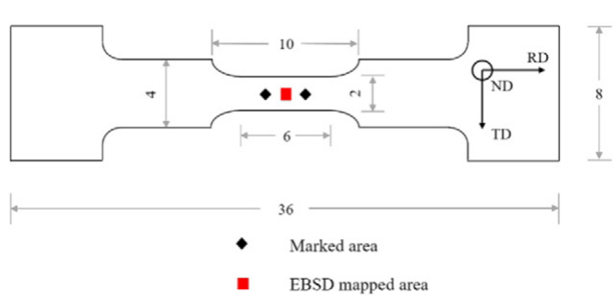

Fig. 1. The specific dimensions (in mm) of the tensile specimen.

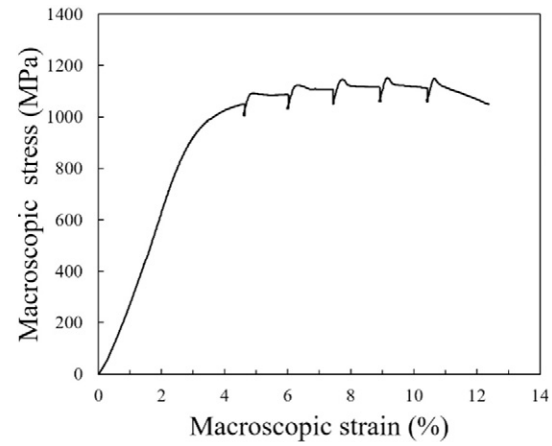

Fig. 2. Macroscopic stress–strain curves of the specimen obtained during in-situ EBSD experiment.

3.2. The volume fractions of RA during the tensile test

The obtained microstructures of the Q&P steel are composed of martensite and RA. Furthermore, based on previous studies of the authors [19], martensite and RA belonged to body-centered cubic (bcc) and face-centered cubic (fcc) structure, respectively. Thus, it is easy to distinguish RA from martensite through ESBD characterization. The volume fractions of RA under varying true strains are presented in Fig. 3. According to this figure, the amount of RA decreases gradually as the true strain increases, which can be attributed to the deformation-induced martensitic transformation of austenite. In other words, austenite would transform partially into martensite owing to the effect of deformation. Such a similar phenomenon was also observed in previous studies [13].

3.3. Deformation behavior of RA under different true strains

The deformation behavior of RA grains under varying true strains was investigated through phase maps and inverse pole figure maps, as shown in Figs. 4–5. Moreover, the microstructural evolution and transformation behavior of three types of RA were also carefully analyzed during the deformation in this study. The first type of RA was located at the triple edges, the second type was positioned within an RA grain with twin faults, and the third type was distributed between the martensite.

Table 1
True strains obtained in in-situ tensile tests for the Q&P steel.

True strain (%)	1.3	2.6	4.0	5.4	6.7	9.1